

Thermal effects in the photoelectron spectra of Na_N^- clusters ($N=4-19$)M. Moseler,^{1,2} B. Huber,² H. Häkkinen,³ U. Landman,³ G. Wrigge,⁴ M. Astruc Hoffmann,⁴ and B. v. Issendorff⁴¹Fraunhofer Institut für Werkstoffmechanik, Wöhlerstrasse 11, 79108 Freiburg, Germany²Theoretische Quantendynamik, Fakultät für Physik, Universität Freiburg, 79106 Freiburg, Germany³School of Physics, Georgia Institute of Technology, Atlanta, Georgia 30332-0430, USA⁴Fakultät für Physik, Universität Freiburg, Hermann-Herder-Strasse 3, 79106 Freiburg, Germany

(Received 18 March 2003; revised manuscript received 6 June 2003; published 23 October 2003)

Photoelectron spectra (PES) of sodium cluster anions Na_N^- ($4 \leq N \leq 19$), measured at close to room temperature, are compared to the electronic density of states obtained from Born-Oppenheimer local-spin-density Langevin molecular-dynamics simulations. Although the shapes of the clusters follow the general predictions of jellium models, considerable deviations occur for the sizes with $N \leq 7$. Most notably, Na_7^- shows a triaxial deformation at elevated temperatures, caused by thermally induced quadrupole shape fluctuations. For Na_{12}^- as well as for Na_{13}^- our simulations confirm the jellium model prediction of the existence of two quasidegenerate (and thermally stable) shape isomers. The experimental PES data of these $1d$ midshell clusters, however, suggest that only the oblate shapes are present in the experiment. This phenomenon may originate from the formation mechanism of the clusters in the beam.

DOI: 10.1103/PhysRevB.68.165413

PACS number(s): 36.40.Cg, 36.40.Mr, 33.60.-q

I. INTRODUCTION

Photoelectron spectroscopy is a frequently used experimental method to extract electronic binding energies from atomic, molecular, and condensed-matter systems. For molecules and clusters at low temperatures, a comparison of the measured photoelectron spectra (PES) with the electronic density of states (DOS) obtained from *ab initio* calculations for $T=0$ optimal structures, provides information about the underlying electronic structure and may lead to assignments of pertinent structures. At finite temperatures floppy systems such as sodium clusters undergo large-amplitude vibrations or even isomerization (in fact, medium-sized sodium clusters actually melt already significantly below room temperature¹). In such a case the PES represent superpositions of the spectra of more or less different structures and therefore yield information about these structures as well as on the isomerization dynamics.

Sodium is one of the best representatives of a free-electron metal, which is the reason why many of the properties of sodium clusters have been successfully described by jellium²⁻⁶ and Clemenger-Nilson⁷ models. Still these models are quite crude approximations, and it is therefore desirable to check their predictions by theoretical and experimental work which yields detailed information about the geometrical and electronic structures of the clusters.

Although more complicated systems such as aluminum⁸ or silicon⁹ cluster anions have already been extensively studied, our knowledge concerning the PES of sodium cluster anions is still limited to cluster sizes below the octamer,¹⁰⁻¹² a surprising fact in view of the significant efforts that has been spent in the past to explore this system.⁷ For instance, it is still unclear whether room-temperature sodium clusters in the middle of the jellium $1d$ shell exhibit a prolate or an oblate shape,³⁻⁶ or rather a coexistence of the two.

We report here on a combined experimental and theoretical study of room-temperature Na_N^- clusters ($N=4-19$). Comparison of measured photoelectron spectra with the elec-

tronic density of states recorded in finite-temperature *ab initio* simulations allows us to extract detailed information about static and dynamic shape properties of simple metal clusters. Although the main features of the PES spectra can be understood through the use of the jellium model, we are able to detect and explain several spectral details. We show that the influence of the ions leads to a slightly prolate shape of the magic eight-electron cluster Na_7^- , and that an additional splitting of jellium p -type lines in the prolate clusters Na_7^- and Na_9^- is caused by thermally induced quadrupole shape fluctuations, clearly observable in the experiment. Furthermore, theoretical studies of $1d$ midshell clusters Na_{12}^- and Na_{13}^- revealed two energetically nearly degenerate oblate and prolate ground states (GS) in agreement with jellium calculations.³⁻⁶ However, the experimental PES of these two clusters can only be interpreted by the oblate shapes. We relate this phenomenon to the formation mechanism of the clusters in the beam.

II. METHODS

For the photoelectron spectroscopy experiments the same apparatus has been used as in a recent study of positively charged sodium clusters.¹³ The clusters are produced in a gas aggregation source, in which sodium is evaporated from a crucible into a liquid-nitrogen-cooled stream of helium having a pressure of about 0.5 mbar. The clusters are ionized by a weak gas discharge burning in the crucible, and thermalized afterwards by collisions with the cold He gas. After expansion into the vacuum the clusters enter a rf octupole ion guide. This octupole extends from the source chamber into the next chamber and has two purposes: it is used to transport a large portion of the clusters through the 3 mm aperture separating the two chambers, and it is used as a temporal trap for the clusters in order to bunch the continuous output of the cluster source. This is achieved by pulsing the exit aperture of the octupole, and enhances the cluster intensity in a bunch by a factor of 10–100. This temporal trapping of the clusters,

which is necessary in order to obtain sufficient intensity for the photoelectron spectroscopy, also leads to an increase of their temperature due to collisions with background gas atoms (mainly helium). The degree of heating of the clusters is difficult to quantify. A rough estimate can be obtained from the intensity of the odd-even modulation visible in the mass spectra. It is comparable to the modulation observed for positively charged clusters with temperatures between 250 K and 300 K; the clusters studied here therefore most probably had temperatures in this range.

After leaving the octupole the clusters enter a high-resolution double-reflectron time-of-flight mass spectrometer, where a single cluster size is selected by a multiwire mass gate. These clusters are decelerated and inserted into a magnetic bottle photoelectron spectrometer, where they are irradiated by an XeCl excimer laser ($h\nu=4.02$ eV). The flight time distribution of the emitted electrons is measured and converted into a binding-energy distribution. The spectrometer has an energy resolution of about $E/dE=40$. It has been calibrated by measuring the known spectrum of Pt^- , which leads to an error of the energy axis of less than 30 meV. In most cases the photoelectron spectra have been averaged over 30 000 laser shots at a repetition rate of 100 Hz.

Our *ab initio* treatment of the sodium cluster anions utilizes the Born-Oppenheimer (BO) approximation for the ionic molecular dynamics (MD) and on density functional theory (DFT) in the framework of the local-spin-density (LSD) approximation for the description of the electronic ground state. The Kohn-Sham (KS) equations of DFT were solved for the sodium $3s$ valence electrons employing the BO-LSD-MD method.¹⁴ Nonlocal pseudopotentials¹⁵ were used to describe the electron-ion interaction. Exchange and correlation were treated within LSD and a fully self-consistent generalized gradient correction (GGA)¹⁶ has been applied.

Finite-temperature trajectories were generated by Langevin MD starting from an arbitrary initial ionic configuration for the Na_N^- clusters. At room temperature all the clusters behave liquidlike¹⁷ and therefore equilibration periods of the order of 5 ps were deemed sufficient to remove the initial-state effects from the ionic trajectories. The subsequent sampling trajectories covered a time period of about 20 ps. Low-energy isomers were determined by frequent quenches of configurations extracted from these trajectories.

For a comparison with the experimental PES, the entire DOS was rigidly shifted in order to align the KS eigenvalue of the highest occupied molecular orbital (ϵ_{HOMO}) of each of the GS clusters with the theoretical vertical detachment energy, obtained directly for the GS cluster in question through a total-energy calculation of the neutral cluster in the geometry of the anion. Such a procedure is analogous to the “generalized Koopman’s theorem”¹⁸ that corrects for the approximations made for the exchange and correlation potential. This method has proven to yield a remarkable agreement between the self-consistently shifted DOS and experimental PES in the case of aluminum⁸ and silicon clusters.⁹

At first, the good correspondence between the calculated DOS and the measured PES might be surprising since most density-functional practitioners consider KS orbitals and en-

ergies as mere auxiliary quantities without a physical meaning; the only exception being the exact KS HOMO level for which the equality of $-\epsilon_{HOMO}$ and the vertical detachment energy is theoretically justified.¹⁹ However, recently the interpretation of the exact Kohn-Sham orbital energies as rather accurate approximations to the vertical ionization potentials has gained strong theoretical support by the rigorous analysis given in Ref. 19, providing a physical basis for the KS orbital energies; in this context exact refers to calculations were the treatment of the exchange and correlation terms goes beyond the standard local-density approximation and/or GGA approximations (see, e.g., Ref. 19).

From the comparison of experimental ionization potentials with exact as well as approximate KS orbital energies reported in Ref. 19, we conclude that most of the deviations of the theoretical DOS from the experimental PES (including the need for a rigid shift of the calculated DOS, as described above) originate from the approximate nature of the exchange and correlation functionals (including gradient corrections) used in this study. Of course, other functionals including for instance, self-interaction corrections²⁰ or higher level calculations²¹ might reduce these deviations, but for an almost-free-electron material such as sodium the agreement between the LSD-DOS and the PES was sufficient enough, and we refrained from additional theoretical refinements.

III. RESULTS AND DISCUSSION

For each size, the lowest-energy structure (perceived ground state²²) is displayed in Fig. 1. The GS structures for $N \leq 5$ (Ref. 23) agree with earlier calculations.¹¹ In most cases other isomers with similar shapes were only slightly higher in energy, e.g., a rhombus structure of Na_4^- (not displayed) was found to be only 20 meV higher in energy than the linear tetramer.²⁴ Starting from the W-shaped pentamer and ending with Na_{11}^- a growth pattern can be identified, i.e., the topology of the Na_N^- cluster derives from Na_{N-1}^- by replacing a particular atom in the structure of Na_{N-1}^- by a dimer (Na_6^- , Na_7^- , and Na_{11}^-), or by capping a facet of the Na_{N-1}^- cluster (Na_8^- , Na_9^- , and Na_{10}^-). Interestingly, our search for the GS structures of the midshell clusters Na_{12}^- and Na_{13}^- resulted in two energetically quasidegenerate GS isomers with clearly different shapes (Na_{12}^- : triaxial oblate vs triaxial prolate; Na_{13}^- : axially symmetric prolate and oblate) confirming corresponding jellium predictions. The structure of Na_{16}^- resembles the GS of Na_{15}^- with the added atom squeezed into the center of the cluster. The highly symmetric GS of Na_{18}^- derives from the C_{4v} GS of Na_{17}^- with an additional atom capping one of the square facets. The GS of Na_{19}^- is not directly derived from that of Na_{18}^- .

The cluster shapes were analyzed by calculating the radii of gyration ($R_{min} \leq R_{middle} \leq R_{max}$) from analysis of the principal moments of inertia for the ionic coordinates. The radii of the GS clusters and the average radii from our finite-temperature simulations are plotted in Figs. 2(a) and 2(b), respectively. They exhibit the same size-evolutionary pattern as already found for a variety of jellium models; see, for instance, the ultimate jellium results⁶ plotted in Fig. 2(c).

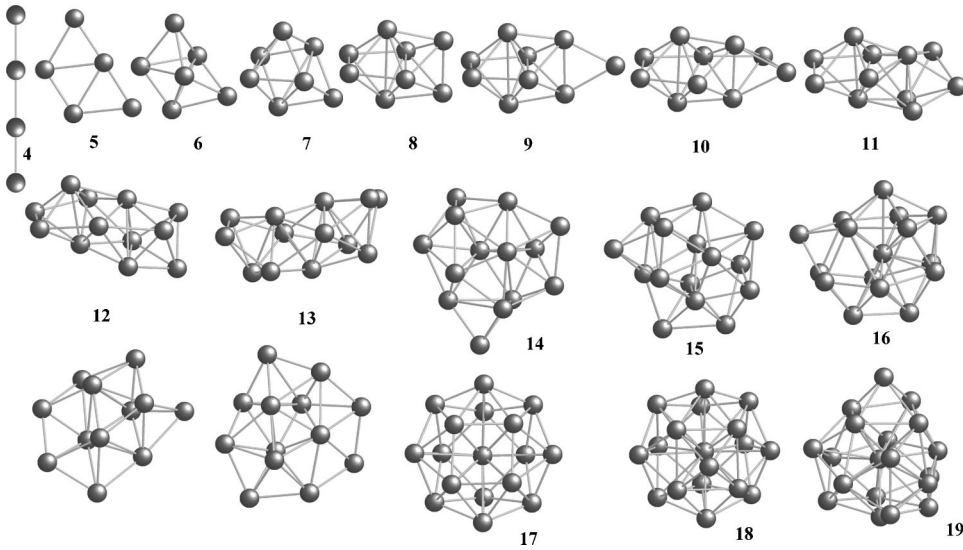


FIG. 1. Ground-state structures of Na_N^- clusters ($N=4-19$). For most sizes energetically close lying isomers were found. For Na_{12}^- and Na_{13}^- , two degenerate isomers with different shapes occur—those in the middle row are prolate and those in the bottom row are oblate.

Here we point out differences between Figs. 2(a), 2(b), and 2(c) that will be helpful for discussing the experimental photoelectron spectra below.

First we remark that the ionic background potential causes the largest deviations between the radii obtained from our BO-LSD-MD calculations and the jellium results for the smallest clusters with $N \leq 7$ (8 or less electrons), e.g., the

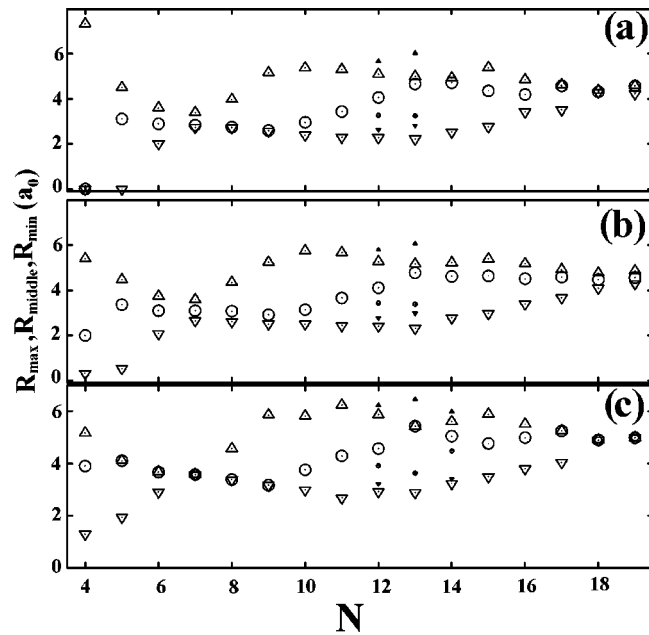


FIG. 2. The three radii (R_{max} , R_{middle} , and R_{min}) of the anionic sodium clusters along the principal axis, plotted vs the number of atoms in the cluster, N . Down-triangles, circles, and up-triangles correspond to R_{min} , R_{middle} , and R_{max} , respectively. The radii were obtained from the moments of inertia of the ionic background. (a) Radii pertaining to the GS structure, see Fig. 1. (b) Thermally averaged radii from room-temperature BO-LSD-MD trajectories. (c) Radii calculated from the reported Hill-Wheeler parameters in the ultimate jellium results (Ref. 6). Small filled symbols in (a) and (c) represents other energetically degenerate GS isomers and in (b) averages over the trajectories in the shape basins of this isomers.

eight-electron cluster Na_7^- has a prolate GS and a triaxial deformation at room temperature in the BO-LSD-MD simulations, whereas the jellium model predicts it to be spherical. Second, the shapes calculated from the BO-LSD-MD results for the larger clusters agree much better with the jellium predictions, especially in the $1d$ midshell. While for Na_{12}^- both isomers exhibit strong triaxial shape deformation (one more oblate, the other more prolate), the Na_{13}^- GS structures are almost ideally oblate and prolate spheroidal. These findings are in excellent agreement with the predictions of the ultimate jellium model⁶ [compare Fig. 2(a) with Fig. 2(c)]. Other jellium models allowing triaxial deformations predict a similar isomerism for the $1d$ midshell.³⁻⁵

In the following, we compare the experimental photoelectron spectra of Na_N^- ($4 \leq N \leq 19$) (see thin solid curves in Fig. 3) with the Gaussian broadened DOS of our GS clusters (thick solid curves in the first and third columns of Fig. 3) and with the DOS from our room-temperature BO-LSD-MD simulations (represented by the stick spectra in the second and fourth columns of Fig. 3). Within the BO-LSD-MD thermal sampling period, the energies of the KS orbitals were recorded and accumulated in bins of width of 25 meV yielding a histogram, and thus a continuous DOS without an artificial Gaussian or Lorentzian broadening.

For low electron binding energies, we observe a good overall agreement between the theoretical DOS's and the experimental data.²⁵ We wish to remark that no additional empirical shifting (see, e.g., Ref. 9) has been applied to the DOS. Such shifts would result in many cases in an even better agreement between the experiment and the simulation. Note that the binding energies of the stronger bound electronic states are consistently overestimated (e.g., the $1s$ state typically by about 0.3 eV) in our simulations. The fact that we observed the same trend in the optical spectra of sodium cluster cations²⁶ leads to the conclusion that the LSD approximation is the likely cause of this effect.

In many cases, the Gaussian broadened DOS of the GS clusters already provides a reasonable description of the measured PES (see, e.g., Na_5^- , Na_6^- , Na_{11}^- , Na_{13}^- oblate, and

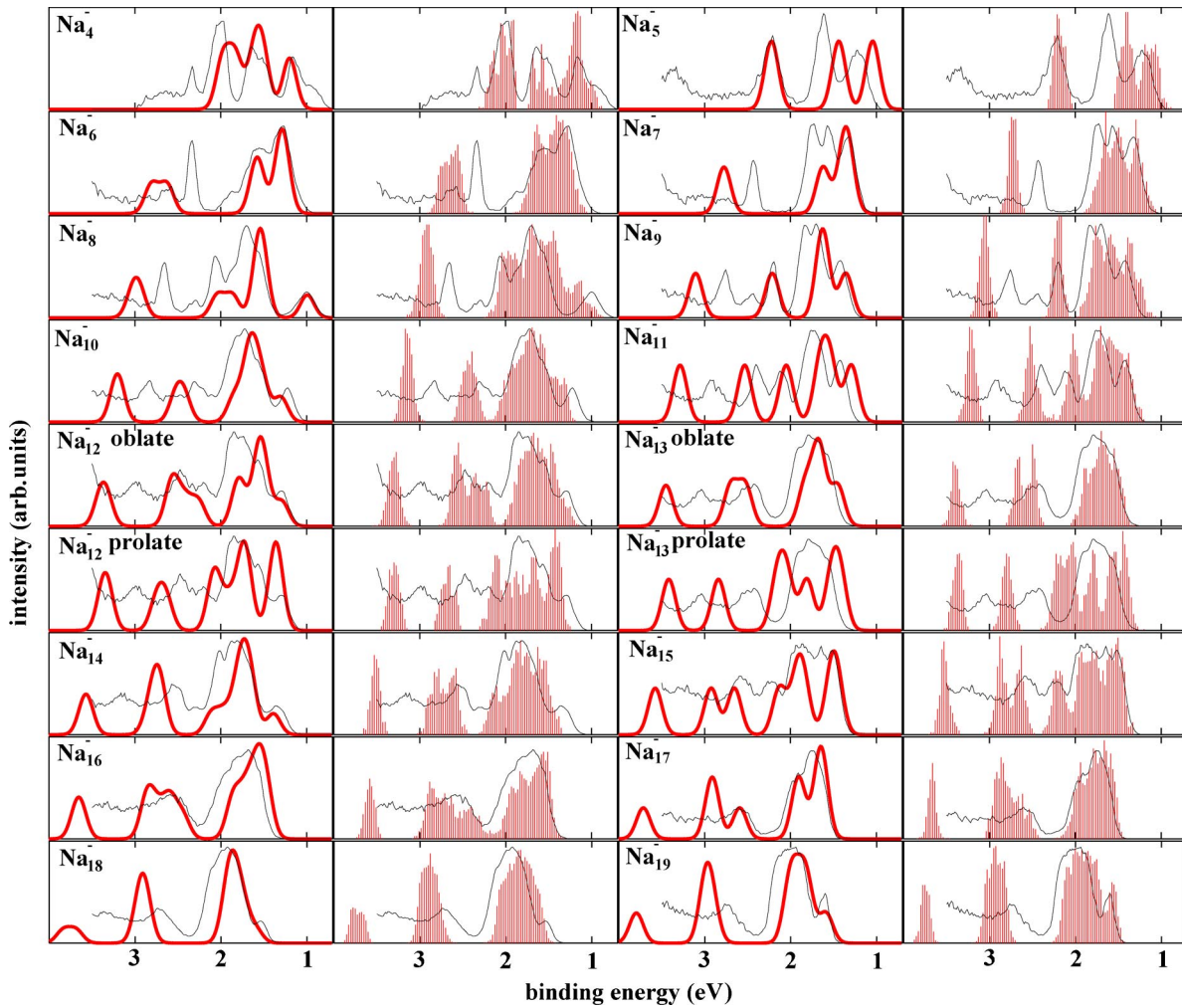


FIG. 3. Experimental photoelectron spectra of sodium cluster anions (thin solid curves) are compared to the Gaussian broadened ($\sigma = 0.08$ eV) ground-state DOS (thick solid curves in the first and third columns), and to the thermally broadened DOS obtained from room-temperature BO-LSD-MD trajectories (histograms in the second and fourth columns).

Na_{16}^-). For other clusters, several details in the spectra are not well reproduced and some are even absent. Notable examples are the splitting of the peak at 1.8 eV binding energy in the spectra of Na_7^- and Na_9^- as well as a poor description of the overall line shapes of these clusters. The reason for this failure is that at room temperature sodium clusters may be considered as liquidlike, consequently, strong deformations occur and basins of several higher-lying isomers are explored (even in our relatively short simulations) resulting in a significant modification of the DOS. For instance, isomerization of the linear Na_4^- GS into the basin of the rhombus structure was observed in our simulations and therefore the thermally broadened DOS reproduces the experimental peak at 2.1 eV much better.

A critical inspection of Fig. 3 reveals that the theoretical 300-K spectra of the anionic clusters with an even number of atoms (open electronic spin shell) shows a lower degree of agreement with the experiment than the odd-numbered Na_N^- clusters (closed spin shell). For the open spin-shell clusters Na_8^- , Na_{10}^- , Na_{12}^- , and Na_{14}^- the GS Gaussian broadened DOS reproduces rather well the lowest-energy peak of the

measured PES, while this peak merges with the first main band at 1.5–2.2 eV in the thermally averaged BO-LSD-MD DOS results. By lowering the temperature in the simulations we can recover this feature; see Fig. 4(a), which shows the thermally averaged DOS obtained from BO-LSD-MD simulation for Na_8^- at 200 K. Since the open spin-shell clusters are most likely less stable than closed spin-shell clusters (the evaporation energy of the monomer shows an odd-even oscillation as a function of the electron number), they can be on average slightly colder in the experimental beam (the clusters are cooled by evaporation of monomers). Comparison of the simulated and measured PES supports this scenario.

According to the jellium model, the eight-electron cluster Na_7^- should be spherical [Fig. 2(c)] reflecting the $1p$ shell closure. However, due to the discrete ionic background the valence electron distribution is slightly prolate deformed leading to a twofold splitting of the threefold degenerate jellium $1p$ shell (see the GS spectrum in Fig. 3). The experimentally observed threefold splitting of the $1p$ shell is reproduced by the finite-temperature simulations where the

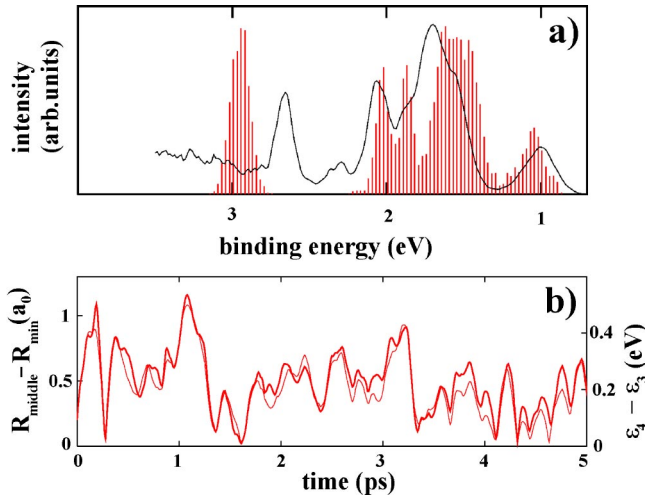


FIG. 4. (a) The DOS of Na₈⁻ obtained from a 200-K BO-LSD-MD trajectory (histogram) compared to the corresponding experimental PES (solid curve). (b) For Na₇⁻: the temporal evolution of $R_{middle} - R_{min}$ (thick solid curve, scale on the left) correlates with the difference of the HOMO and the HOMO-1 eigenvalues ($\epsilon_4 - \epsilon_3$) (thin solid curve, scale on the right).

thermal ionic motion causes dynamical quadrupole deformations. These can be correlated to the lifting of the remaining degeneracy in the $1p$ shell, as displayed in Fig. 4(b) which shows the time evolution of the difference between the cluster's median (R_{middle}) and the minimum (R_{min}) radius as well as the difference between the HOMO and the HOMO-1 eigenvalues ($\epsilon_4 - \epsilon_3$).

This striking correlation between the geometrical arrangement of the ions and the electronic structure can already be explained in the framework of the simple Clemenger-Nilsson model (for a review, see Ref. 7), where the electronic potential of the cluster is treated as an ellipsoidal harmonic confinement (with principal radii R_x , R_y , and R_z) yielding a simple expression for the electronic eigenvalues,

$$E_{n_x, n_y, n_z} = \hbar \omega_0 \left[\left(n_x + \frac{1}{2} \right) \frac{R_0}{R_x} + \left(n_y + \frac{1}{2} \right) \frac{R_0}{R_y} + \left(n_z + \frac{1}{2} \right) \frac{R_0}{R_z} \right].$$

Here, $\omega_0/2$ denotes the curvature of the spherical harmonic confinement (that is, when $R_x = R_y = R_z$) and the value of R_0 is determined by volume conservation, i.e., $R_0^3 = R_x R_y R_z$. After a small triaxial deformation, we may assume that $R_x < R_y < R_z$ (while keeping the volume unchanged), and therefore the eight electrons of Na₇⁻ occupy four orbitals with $\epsilon_1 = E_{0,0,0} < \epsilon_2 = E_{0,0,1} < \epsilon_3 = E_{0,1,0} < \epsilon_4 = E_{1,0,0}$. Consequently, the eigenvalue difference

$$\epsilon_4 - \epsilon_3 = \frac{\hbar \omega_0 R_0}{R_x R_y} (R_y - R_x)$$

correlates with $R_y - R_x = R_{middle} - R_{min}$, in perfect agreement with the finding in Fig. 4(b).

The triaxial shape and the concomitant threefold splitting of the $1p$ shell at elevated temperatures have been previously predicted by BO-LSD-MD simulations for the neutral magic

Na₈ cluster,²⁷ as well as in a simulation of the PES of Cu₇⁻.²⁸ The same mechanism operates here also for Na₉⁻ with its axial symmetric GS and triaxial room-temperature shape.

Since the $T=0$ shape isomers for Na₁₂⁻ and Na₁₃⁻ are energetically almost degenerate, one may expect that Na₁₂⁻ as well as Na₁₃⁻ would visit both the oblate and the prolate basins at finite temperature, leading to a mixture of the characteristic features of the GS DOS (see thick solid lines in the panels marked oblate and prolate in Fig. 3). One consequently would expect strongly broadened experimental spectra for these clusters. However, in the BO-LSD-MD simulations trajectories that started from the oblate or prolate basins stayed within those basins for tens of picoseconds, indicating that there has to be a sizable barrier between them at room temperature. This result agrees with earlier BO-LSD-MD simulations of the neutral midshell Na₁₄ cluster which showed stable oblate and prolate shape deformations in a 10 ps time scale at temperatures over 600 K.²⁷

The experimental PES of both Na₁₂⁻ and Na₁₃⁻ can only be interpreted by the simulated *oblate* DOS spectra (Fig. 3) which is a strong indication that only one shape isomer is favored when those clusters are formed in the experiment. A possible explanation for that is that the mid-shell Na₁₂⁻ and Na₁₃⁻ clusters, formed by evaporation of monomers from the slightly larger parent clusters (which are *oblate*, see Fig. 2) still reflect the shapes of their parents, coupled with the significant barrier for the thermally induced shape change as observed in our simulations.

A barrier crossing from one shape basin to another can even involve a momentary spin flip. It is well known that lifting the degeneracy and optimizing the total energy for the $1d$ midshell clusters may involve one of the two following mechanisms: (i) maximizing the cluster spin while keeping a close-spherical shape of the valence electron distribution (a cluster analog to the Hund's rule of atoms) or (ii) deforming the shape and minimizing the spin (i.e., maximum spin coupling of the electrons). Since clusters are inherently deformable by thermal motion of the ions, mechanism (ii) is commonly assumed. However, we have also studied the possibility of the maximum spin mechanism (i), by starting a BO-LSD-MD simulation from an icosahedral Na₁₃⁻ with a septet spin $S=3$ (the spin isomer of the icosahedron with the lowest energy at $T=0$) and heating the cluster to 300 K. The cluster deformed to an oblate shape and the spin spontaneously flipped to the $S=1$ triplet. This shape and spin configuration was stable for 30 ps yielding a similar and only slightly broader PES than the oblate singlet $S=0$ trajectory shown in Fig. 3.

IV. CONCLUSIONS

In summary, a combination of photoelectron spectroscopy and finite-temperature *ab initio* molecular-dynamics calculations has been used to identify the structures of negatively charged sodium clusters with 4–19 atoms. While the overall

shapes of the larger clusters ($N > 7$) are in almost perfect agreement with jellium model predictions, exceptions occur for the size range $N = 4-7$ where, for instance, the magic Na_7^- cluster exhibits a triaxial deformation in our finite-temperature simulations. Nevertheless, the results demonstrate once more how well sodium clusters can be described by the simple jellium model.

ACKNOWLEDGMENTS

This work was supported by the Deutsche Forschungsgemeinschaft (MM,BvI), the Academy of Finland (H.H.) and the U.S. Department of Energy (U.L.). Computations were done on Cray T3E at NIC Jülich and HLRS Stuttgart.

-
- ¹M. Schmidt, R. Kusche, B.V. Issendorff, and H. Haberland, *Nature* (London) **393**, 6682 (1998).
- ²W. Ekardt, *Phys. Rev. Lett.* **52**, 1925 (1984).
- ³G. Lauritsch, P.-G. Reinhard, J. Meyer, and M. Brack, *Phys. Lett. A* **160**, 179 (1991).
- ⁴S. Frauendorf and V.V. Pahkevich, *Z. Phys. D: At., Mol. Clusters* **26**, 98 (1993).
- ⁵C. Yannouleas and U. Landman, *Phys. Rev. B* **48**, 8376 (1993); **51**, 1902 (1995); *J. Phys. Chem.* **102**, 2505 (1998).
- ⁶M. Koskinen, P.O. Lipas, and M. Manninen, *Z. Phys. D: At., Mol. Clusters* **35**, 285 (1995).
- ⁷W. deHeer, *Rev. Mod. Phys.* **65**, 611 (1993).
- ⁸J. Akola, M. Manninen, H. Hakkinen, U. Landman, X. Li, and L.-S. Wang, *Phys. Rev. B* **60**, 11 297 (1999).
- ⁹L. Kronik, R. Fromherz, E. Ko, G. Ganteför, and J.R. Chelikowsky, *Nat. Mater.* **1**, 1 (2002).
- ¹⁰K.M. McHugh, J.G. Eaton, G.H. Lee, H.W. Sarkas, L.H. Kidder, J.T. Snodgrass, and K.H. Bowen, *J. Chem. Phys.* **91**, 3792 (1989).
- ¹¹V. Bonacic-Koutecky, V.P. Fantucci, and J. Koutecky, *J. Chem. Phys.* **91**, 3794 (1989).
- ¹²G. Ganteför, A. Handschuh, H. Möller, C.Y. Cha, P.S. Bechtold, and W. Eberhard, *Surf. Rev. Lett.* **3**, 399 (1996).
- ¹³G. Wrigge, M. Astruc Hoffmann, and B.v. Issendorff, *Phys. Rev. A* **65**, 063201 (2002).
- ¹⁴R. Barnett and U. Landman, *Phys. Rev. B* **48**, 2081 (1993).
- ¹⁵N. Troullier and J.L. Martins, *Phys. Rev. B* **43**, 1993 (1991); The core radii (in units of a_0) are s (2.45) and p (2.6), with p the local component. A plane-wave basis with a 10-Ry cutoff was used.
- ¹⁶J.P. Perdew, K. Burke, and M. Ernzerhof, *Phys. Rev. Lett.* **77**, 3865 (1996).
- ¹⁷All calculated Lindemann indices of our 300-K trajectories were larger than 16%.
- ¹⁸D.J. Tozer and N.C. Handy, *J. Chem. Phys.* **108**, 2545 (1998); **109**, 10 180 (1998).
- ¹⁹D.P. Chong, O.V. Gritsenko, and E.J. Baerends, *J. Chem. Phys.* **116**, 1760 (2002); O.V. Gritsenko and E.J. Baerends, *ibid.* **117**, 9154 (2002).
- ²⁰J.P. Perdew and M.R. Norman, *Phys. Rev. B* **26**, 5445 (1982).
- ²¹S. Saito *et al.*, *J. Phys.: Condens. Matter* **2**, 9041 (1990).
- ²²The number of stable cluster isomers increases exponentially with clusters size, consequently, the search for the global energy minimum becomes more difficult for larger clusters. We presume that the lowest energy structures obtained from the simulated annealing treatment described in the text are representative of the true ground state clusters which may be prohibitively difficult to find for sizes $N \geq 10$.
- ²³Attempts to converge Na_N^- for $N < 4$ using LSD/GGA resulted in an unbound (and thus unphysical) KS HOMO orbital.
- ²⁴See also Fig. 1 in H. Häkkinen, M. Moseler, and U. Landman, *Phys. Rev. Lett.* **89**, 033401 (2002) for the low-energy isomers of Na_7^- .
- ²⁵Note that the DOS for Na_4^- and Na_5^- is also in remarkable agreement with the CI calculations of Bonacic-Koutecky *et al.* (Ref. 11) Solely, the small feature in the experimental PES of Na_4^- near 2.2 eV binding energy is reproduced by the configuration-interaction calculation while it seems to be merged with a neighboring peak in the DFT-DOS.
- ²⁶M. Moseler, H. Häkkinen, and U. Landman, *Phys. Rev. Lett.* **87**, 053401 (2001).
- ²⁷H. Häkkinen and M. Manninen, *Phys. Rev. B* **52**, 1540 (1995).
- ²⁸C. Massobrio, A. Pasquarello, and R. Car, *Phys. Rev. B* **54**, 8913 (1996).